AIP Review of Scientific Instruments

Considerations for capacitance DLTS measurements using a lockin amplifier

F. D. Auret

Citation: Review of Scientific Instruments **57**, 1597 (1986); doi: 10.1063/1.1138537
View online: http://dx.doi.org/10.1063/1.1138537
View Table of Contents: http://scitation.aip.org/content/aip/journal/rsi/57/8?ver=pdfcov
Published by the AIP Publishing

Considerations for capacitance DLTS measurements using a lock-in amplifier

F. D. Auret

Department of Physics, University of Port Elizabeth, P. O. Box 1600, Port Elizabeth, 6000, Republic of South Africa

(Received 9 December 1985; accepted for publication 16 April 1986)

An outline is presented of how to numerically account for the gate-off time, consisting of both the pulse width and delay times, when performing lock-in amplifier based capacitance deep level transient spectroscopy (DLTS) measurements at frequencies up to 2000 Hz. This frequency is about ten times higher than the maximum frequency normally used for these measurements when using 1-MHz capacitance meters. Further, the relationship between the frequency, pulse width, and delay time was established for which the commonly used value of the normalized thermal emission decay time constant τ_{max}/T_0 may be assumed constant ($=0.424$) without introducing observable errors in the defect parameters calculated from DLTS data. Because the effect of measuring at higher frequencies is to shift the DLTS peaks to higher temperatures, it was found that when using frequencies between 50 and 2000 Hz, defects such as the E2 level in radiation-damaged GaAs, which are usually observed below 77 K at frequencies below 50 Hz, may be conveniently and accurately characterized by capacitance DLTS at temperatures above that of liquid nitrogen.

INTRODUCTION

In recent years deep level transient spectroscopy (DLTS)[1] has become an increasingly important technique for characterizing defects in semiconductors. This technique is based upon the analysis of capacitance or current transients caused by thermal emission of carriers from defect levels in the depletion region of a rectifying semiconductor junction. The first DLTS results, reported by Lang in 1974,[1] were obtained by using a dual-channel boxcar averager for establishing a "rate window" in order to analyze the transient. Shortly thereafter, the use of an exponential correlator[2] and lock-in amplifier[3] were proposed as alternatives for the boxcar. In each of these cases the most important problem is to extract the DLTS rate window, and, hence, the defect parameters, from the instrument.

Despite the fact that these methods are more time consuming than the more recently developed multiple-gate boxcar methods[4] or methods which employ direct numerical analysis of the transient,[5] the lock-in amplifier (LIA) and boxcar DLTS systems still remain popular because of their ease of operation, their high S/N (signal-to-noise) ratios, the fact that they can be constructed almost entirely from "off-the-shelf" components, and because they do not require sophisticated computing facilities. It has been pointed out[6] that neither the LIA nor boxcar method, however, stands out as the "best" method, and that in the end, the choice of a rate window system is based on personal preference and on the best utilization of existing laboratory equipment.

When using a LIA, the part of the capacitance meter output signal due to the filling pulse and meter's response time (delay time) is gated off by using a sample-and-hold circuit[7] before passing it into the LIA. The result is that part of the signal that enters the LIA is not exponential. The degree of this nonexponentiality is determined by the gate-off time relative to the period at which the LIA operates. The effect of this gate-off time can be corrected for in one of two ways. Firstly, a two-phase lock-in analyzer may be used in the *I–Q* mode,[8] so that only the second and fourth quadrants of the transient are analyzed. This completely eliminates the gate-off effect as long as the gate-off time is less than 1/4 times the LIA period. Secondly, the gate-off effect may be accounted for mathematically by a detailed Fourier analysis of the signal entering the LIA.

In initial studies in which the gate-off time was ignored, the relationship between the maximum emission decay time constant τ_{max} at a DLTS peak and the LIA frequency f was determined as $\tau_{max}=0.42/f$, independent of the gate-off time.[9] In a more detailed study Day *et al.*[6] showed that frequency-dependent errors are introduced when calculating τ_{max} as above, if the gate-off effect is ignored. This leads to incorrect activation energies as calculated from conventional DLTS Arrhenius plots. On the other hand, they found that, if numerically accounted for, the gate-off effect had no influence on the calculated activation energies for their measurements performed in the 5–80-Hz frequency range. In their analysis the gate-off time of 1.6 ms consisted of the capacitance meter response time only and they did not make provision for including the width of the filling pulse in this gate-off time, probably because it was only 20 μs and therefore negligible when compared with the total gate-off time of 1.6 ms.

Most commercially purchased 1-MHz capacitance meters that are used for DLTS cannot pass filling pulses, of which the widths are negligible with respect to the meter's response times, through their internal circuitry. The Boonton 72B and 72BD are probably the most widely used capacitance meters for this purpose and their response times, which are usually $\geqslant 1$ ms, may be reduced to below 200 μs by a few simple modifications.[10] However, they still cannot pass pulses narrower than 50 μs through their circuitry if both the bias and pulse are applied to their rear bias terminals. This method of applying both the bias and the pulse as a single signal to the rear terminals of the capacitance meter offers the convenience of using a single (often programmable) signal generator. If pulses narrower than $50\,\mu s$ are to be used, then they are usually applied to the front terminals of the capacitance meter via a pulse transformer.[7]

In the past, LIA-based DLTS measurements using 1-MHz capacitance meters were usually limited to the 1–200-Hz range. In order to extend this frequency range by increasing the measurement frequency, the part of the transient which is gated off by the sample-and-hold circuit should be as short as possible. It is the purpose of this paper to show that by ignoring the contribution of the pulse width to this gate-off time, large errors in τ_{max} are introduced. The magnitude of these errors increase to above the experimental error limits if the pulse width becomes comparable in size with the delay time and if the frequency is greater than about 0.2/(gate-off time). This in turn leads to errors in the defect properties calculated by using these incorrect values of τ_{max}. The results to be presented will also show that DLTS measurements using 1-MHz capacitance meters can be performed at frequencies up to 2000 Hz, if the capacitance meter is modified so that its response time is less than 0.2 ms and provided both the pulse width and delay time are accounted for when calculating the τ_{max}.

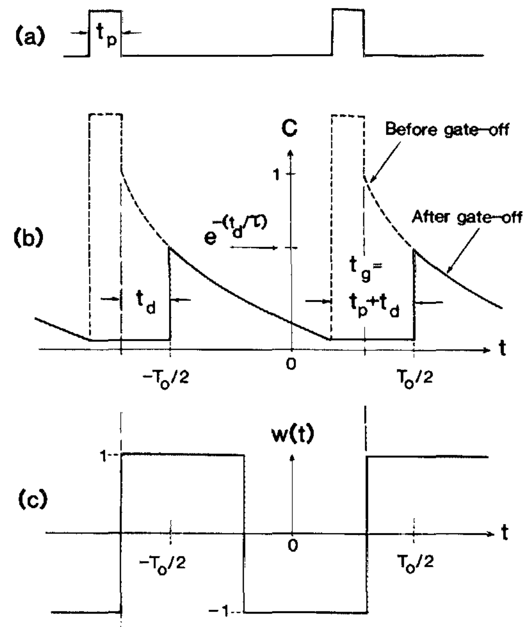

FIG. 1. Phase setting for the "bias-pulse phase reference" mode: (a) filling pulse of width t_p and frequency $f = 1/T_0$; (b) normalized exponential capacitance transient before (broken curve) and after gate-off (solid curve); (c) lock-in amplifier weighting function set in phase with the falling edge of the filling pulse.

I. THEORY

The tuning procedure, signal response, and calculation of defect concentrations from DLTS peak heights obtained from the LIA output have been discussed previously for the ideal case where the filling pulse width t_p and system response time (also referred to as delay time) t_d are negligible when compared to the time between pulses T_0 ($=1/f$).[9] The shortcomings of this analysis were pointed out by Day *et al.*[6] who presented a more detailed analysis in which the system response time t_d was taken into consideration when calculating the LIA output, phase settings, and decay time constants. It will now be shown that it may not always be possible to neglect the width of the filling pulse t_p as was done in their analysis.

In the analysis that follows, the total gate-off time t_g is assumed to consist of two components, namely, the pulse width t_p and the capacitance meter's response time t_d. In order to evaluate the influence of each of these components on the calculated value of τ_{max}, a Fourier analysis of the signal entering the LIA was performed, keeping both t_p and t_d independently variable. Because the "bias-pulse phase-reference" mode[6] was shown to be the least dependent on the LIA phase setting, it was used for the analysis presented here. This mode is illustrated in Fig. 1, and corresponds to the lock-in zero crossing being set at the end of the bias pulse [Figs. 1(a) and 1(c)]. Note that the transient entering the LIA starts at $t = t_d + t_p$ after the rising edge of the pulse. The LIA, for which the pulsing sequences are shown in Fig. 1, registers the phase and first Fourier component of the waveform drawn as a solid line in Fig. 1(b). The LIA response S_{exp} to this partially exponential waveform, is the integral of the product of the LIA square-wave weighting function [Fig. 1(c)] and the first Fourier component of the waveform. For calibration purposes, the ratio S of the LIA's response to a square wave, of the same period S_{sq} to S_{exp} is required:

$$S = S_{sq}/S_{exp}\,. \tag{1}$$

However, since S_{sq} is independent of τ, only S_{exp} will be considered in the analysis that follows.

To calculate the first Fourier component of the waveform in Fig. 1(b), the input signal to the LIA is written as

$$f(t) = \begin{cases} \exp(-t_d/\tau)\exp[-(t+T_0/2)/\tau]\,, \\ -T_0/2 \leqslant t < T_0/2 - t_g \\ \exp(-t_d/\tau)\exp[-(T_0-t_g)/\tau]\,, \\ T_0/2 - t_g \leqslant t < T_0/2 \end{cases} . \tag{2}$$

The Fourier expansion of this function over the interval

$$-T_0/2 \leqslant t < T_0/2$$

is

$$f(t) = \frac{a_0}{2} + \sum_{n=1}^{\infty}\left[a_n \cos\left(\frac{2\pi nt}{T_0}\right) + b_n \sin\left(\frac{2\pi nt}{T_0}\right)\right]. \tag{3}$$

In Eq. (3), a_n and b_n are the Fourier coefficients given by

$$a_n = \left(\frac{2}{T_0}\right)\int_{-T_0/2}^{T_0/2} f(t)\cos\left(\frac{2\pi nt}{T_0}\right)dt \tag{4}$$

and

$$b_n = \left(\frac{2}{T_0}\right)\int_{-T_0/2}^{T_0/2} f(t)\sin\left(\frac{2\pi nt}{T_0}\right)dt\,. \tag{5}$$

For the signal in Fig. 1(b), defined by Eq. (2), the first Fourier coefficients are obtained from Eqs. (4) and (5) with $n = 1$

$$
\begin{aligned}
a_1 = {} & (T_0/2\tau)\exp[-(T_0-t_p)/\tau][\pi^2+(T_0/2\tau)^2]^{-1} \\
& \times\{\cos(2\pi t_g/T_0)-(T_0/2\pi\tau) \\
& \times\sin(2\pi t_g/T_0)-\exp[(T_0-t_g)/\tau]\}
\end{aligned} \tag{6}
$$

and

$$
\begin{aligned}
b_1 = {} & \pi\exp[-(T_0-t_p)/\tau]^{-1}[\pi^2+(T_0/2\tau)^2]^{-1} \\
& \times\{1-(T_0/2\pi\tau)\sin(2\pi t_g/T_0)+(T_0/2\pi\tau)^2 \\
& \times[1-\cos(2\pi t_g/T_0)]-\exp[(T_0-t_g)/\tau]\}\,.
\end{aligned} \tag{7}
$$

The first Fourier component of the signal analyzed by the LIA is thus

$$f_1(t)=a_1\cos(2\pi t/T_0)+b_1\sin(2\pi t/T_0)\,, \tag{8}$$

with a_1 and b_1 given by Eqs. (6) and (7). The LIA response to the incoming signal is obtained from

$$S_{\exp}=\int_{-T_0/2}^{T_0/2} f_1(t)w(t)dt\,,$$

where $w(t)$ is the LIA weighting function shown in Fig. 1(c). By taking into account the boundary conditions for the different sections of the waveform in Fig. 1(b), the LIA output becomes

$$
\begin{aligned}
S_{\exp} = {} & \int_{-T_0/2}^{-t_d} f_1(t)(+1)dt+\int_{-t_d}^{T_0/2-t_d} f_1(t)(-1)dt \\
& +\int_{T_0/2-t_d}^{T_0/2} f_1(t)(+1)dt\,.
\end{aligned} \tag{9}
$$

Equations (8) and (9) result in

$$S_{\exp}=(2T_0/\pi)[a_1\sin(2\pi t_d/T_0)+b_1\cos(2\pi t_d/T_0)]\,, \tag{10}$$

with a_1 and b_1 given by Eqs. (6) and (7). In order to obtain the maximum value of the decay time constant $\tau_{\max}$, the condition for a maximum of the DLTS peak is used

$$dS_{\exp}/d\tau=0\,. \tag{11}$$

The resulting equation, which is obtained by using Eqs. (6), (7), (10), and (11) is given by Eq. (A3) in the Appendix, and was solved numerically for ξ ($=T_0/2\tau_{\max}$) by using the Newton–Raphson iterative method. For most combinations of t_p, t_d, and T_0, convergence was obtained after four or five iterations.

II. RESULTS AND DISCUSSION

A. Theoretical calculations

All the calculations were done for the frequencies from 1 Hz upwards. However, only the results for $f \geqslant 10$ Hz are shown because, with the exception of a few cases, all the calculated values of $\tau_{\max}/T_0$ were equal to 0.424 for frequencies below 10 Hz. In Fig. 2 the variation of $\tau_{\max}/T_0$ with frequency is shown for two cases: $t_d=0$, $0 \leqslant t_p \leqslant 3.2$ ms [Fig. 2(a)] and $t_p=0$, $0 \leqslant t_d \leqslant 3.2$ ms [Fig. 2(b)]. Although these are both idealized cases, they serve the purpose of illustrating the influence of increasing frequency on $\tau_{\max}/T_0$ if either of t_p or t_d is changed while the other is held constant. These sets of curves will also form the basis of some further discussion later in the paper. For all the t_p curves in Fig. 2(a) it is evident that when $t_d=0$, an increase in frequency leads to a monotonic decrease in $\tau_{\max}/T_0$. The curves for different t_p values appear to have the same form except that they shift to lower frequencies as t_p is increased. For all these curves it is seen that the deviation of $\tau_{\max}/T_0$ from 0.424 will be less than 2.5% if $t_p < T_0/5$. On the other hand, the t_d curves in Fig. 2(b) show that for $t_p=0$, $\tau_{\max}/T_0$ first increases and then decreases with increasing frequency. The maximum that they reach corresponds to a 5% deviation from 0.424 and occurs at about $f=0.14/t_d$. At frequencies above $f=0.24/t_d$, the $\tau_{\max}/T_0$ values become 5% less than 0.424 and thereafter decrease sharply. As above, the general shapes of the curves are the same for all t_d values, but they are displaced to lower frequencies if t_d is increased. Note that in Fig. 2(b) the curve for $t_p=0$ and $t_d=1.6$ ms corresponds to the case investigated by Day *et al.* in the range $5 \leqslant f \leqslant 80$ Hz.

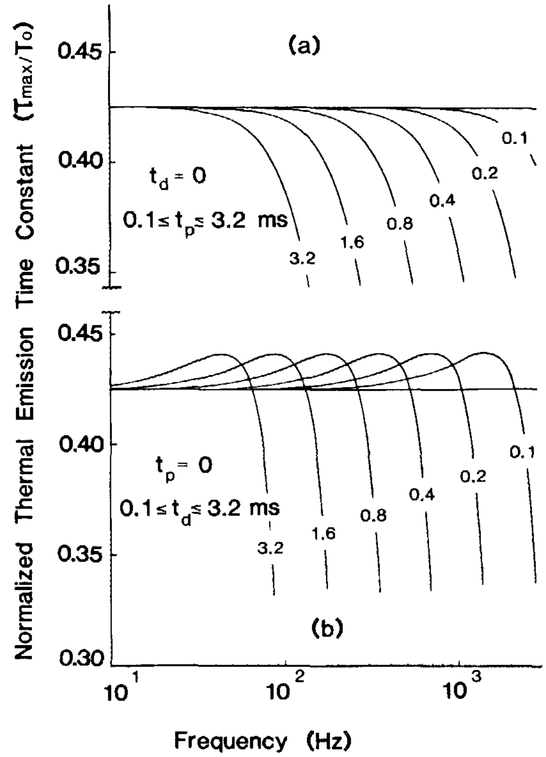

FIG. 2. Normalized maximum emission time constant $\tau_{\max}/T_0$ vs frequency f. (a) $t_d=0$; $0 \leqslant t_p \leqslant 3.2$ ms, (b) $t_p=0$; $0 \leqslant t_d \leqslant 3.2$ ms.

Next, a few combinations of t_p and t_d that would apply to capacitance meters with fast, medium, and slow response times, respectively, are considered. In Fig. 3 the solutions for $\tau_{\max}/T_0$ for such t_p and t_d combinations are shown for frequencies up to 3000 Hz, while Fig. 4 depicts the normalized LIA output of the corresponding t_p and t_d combinations. For a capacitance meter with a fast response time t_p and t_d were chosen to be $\leqslant 0.1$ ms. It is instructive to note that for $t_d=0.1$ ms at 3000 Hz, the values of $\tau_{\max}/T_0$ obtained when ignoring the pulse width, i.e., $t_p=0$, differ from those where $t_p=0.025$ and $t_p=0.05$ ms by 11% and 25%, respectively.

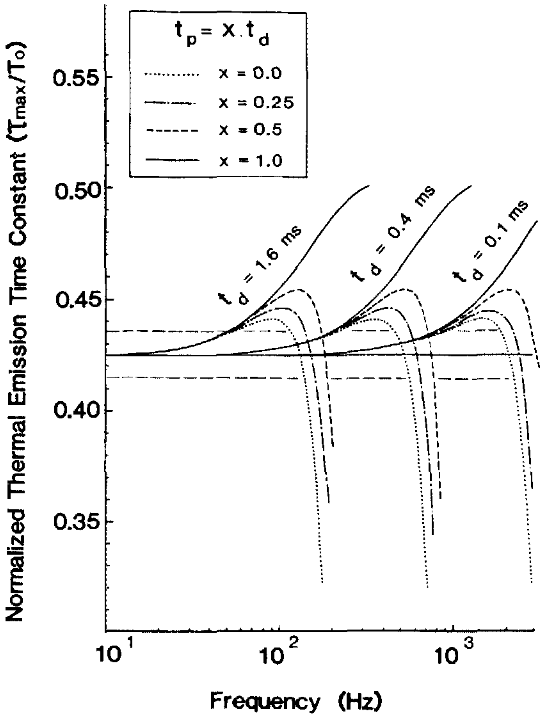

FIG. 3. Normalized maximum emission time constant τ_{max}/T_0 vs frequency for different delay times $t_d = 0.1$, 0.4, and 1.6 ms. For each t_d value, t_p values defined by $t_p = xt_d$ are drawn, with x varying between 0 and 1. The distance between the two broken lines parallel to $\tau_{max}/T_0 = 0.424$ represent a 5% change in the value of τ_{max}/T_0.

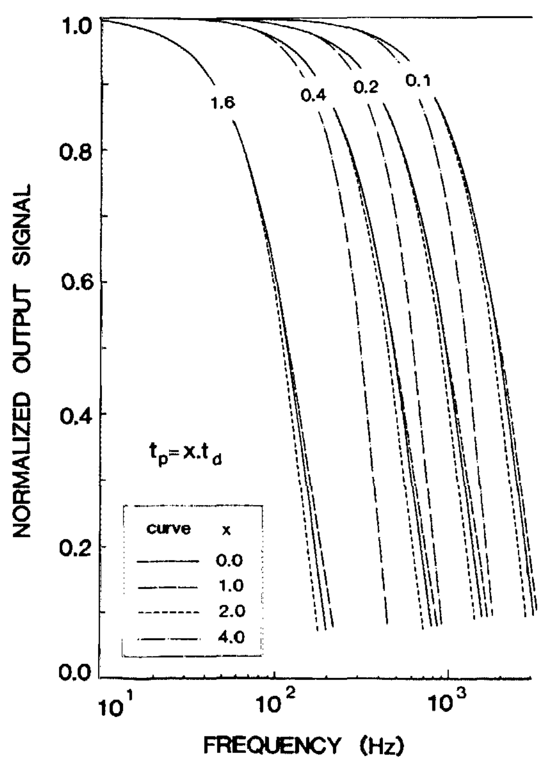

FIG. 4. Normalized lock-in amplifier output vs frequency for $t_d = 0.1$, 0.2, 0.4, and 1.6 ms. For each t_d value, the curves for $t_p = 0$, t_d, $2t_d$, and $4t_d$ are shown.

Thus, for these cases the τ_{max}/T_0 values obtained by neglecting t_p will adversely affect the accuracy of the activation energies and capture cross sections calculated by using them. From Figs. 3 and 4 it can therefore be concluded that accurate defect characterization is possible at frequencies up to 3000 Hz without reducing the normalized LIA output to below 0.2, provided both t_p and t_d are accounted for and, of course, if the capacitance meter is fast enough.

For a medium-speed capacitance meter t_p and t_d were chosen within the ranges $0.1 \leqslant t_p \leqslant 0.4$ ms and $0.2 \leqslant t_d \leqslant 0.4$ ms. The τ_{max}/T_0 curves for $t_d = 0.4$ and $t_p = 0$, 0.1, 0.2, and 0.4 ms are depicted in Fig. 3. As an example, consider the case where $t_p = t_d = 0.4$ ms. Theoretically, the maximum frequency at which measurements are possible for this case should be 1250 Hz. However, in that case, the LIA output would be zero because the entire transient is gated off. From Fig. 4 it is seen that for this t_p and t_d combination the upper frequency limit that can be achieved without decreasing the normalized LIA output signal to below 0.1 must be less than 700–800 Hz. Again the effect of neglecting t_p in the calculation of τ_{max} is obvious from Fig. 3. For $t_p = t_d = 0.4$ ms at 700 Hz a 30% error is made in τ_{max}/T_0 when t_p is ignored. Using similar arguments it may be seen that the maximum practical frequency for $t_d = 0.2$ and $t_p = 0.1$ ms is about 1500 Hz, while if t_d is reduced to 0.15 ms, this frequency increases to about 2000 Hz. The results that will be reported for experimental measurements will be for these values of t_p and t_d, among others.

To enable a comparison to be made between the present work and that of Day *et al.*, the results for a slow capacitance meter for which $t_d = 1.6$ ms, are also included. It is assumed that pulses of between 0 and 3.2 ms can be applied to the DUT (device under test). On the scale in Fig. 3 the curves for $t_p = 0$ and $t_p = 0.02$ ms are indistinguishable. This case corresponds to the results presented by Day *et al.*, who neglected the contribution of their 20-μs pulse width to the gate-off time. It is evident that for this t_p and t_d combination, t_p may be neglected without influencing the calculated τ_{max}/T_0 value. Even for $t_p = 0.2$ ms only a small change in τ_{max}/T_0 is observed when comparing it to the case where $t_p = 0$ (3% at 150 Hz). However, for larger values of t_p, such as 0.4 ms, there is a definite deviation from the zero pulse width case (7% at 150 Hz).

From the three sets of curves in Fig. 3, it is seen that for $t_g > 0.1T_0$, t_p may not be ignored without leading to incorrect τ_{max}/T_0 values unless $t_p < t_d/5$. Further, apart from special cases that will be discussed below, the curves in Fig. 3 showed that the approximation $\tau_{max}/T_0 = 0.424$ is valid to within 1% and 5% for gate-off widths such that $t_g < 0.04T_0$ and $t_g < 0.1T_0$, respectively.

Another interesting observation from Figs. 2(a) and 2(b) is that within a certain frequency range the deviations of τ_{max}/T_0 from their low-frequency limits of 0.424 occur in opposite directions. Although the components in Figs. 2(a) and 2(b) do not add linearly to obtain the final value of τ_{max}/T_0, it is intuitively felt that, because of this opposing influence, the variation in τ_{max}/T_0 may be reduced by appropriate choices of t_p and t_d. The effect observed when varying t_p while keeping t_d constant is illustrated in Fig. 5

for $t_d = 0.1$ and 0.4 ms. Note that in Fig. 5 the τ_{max}/T_0 scale is more sensitive than that of Fig. 3 by a factor of 8. First consider the case of $t_d = 0.1$ ms, applicable to fast capacitance meters. It is evident from Fig. 5 that by increasing t_p from $2t_d$ to $3.5t_d$, the deviation in τ_{max}/T_0 from 0.424 at 500 Hz reduces from 2.5% to 0.5%, which is less than the normal experimental error limits. Thus, for $t_d = 0.1$ and $t_p = 0.35$–0.40 ms, the value of τ_{max}/T_0 may be taken as 0.424 throughout the frequency range $f \leqslant 500$ Hz (i.e., $t_g < 0.2T_0$), without introducing observable errors in the calculated activation energy. The same phenomenon is observed for larger t_d values. For example if $t_d = 0.2$ or 0.4 ms, then a choice of $t_p = 3.5t_d$ would lead to frequency-independent values of $\tau_{max}/T_0 = 0.424$ up to frequencies up to 280 or 150 Hz, respectively.

When estimating the highest frequency at which capacitance DLTS data can be recorded, three factors should be considered. The first is the response time of the capacitance meter. A standard 1-MHz Boonton 72B or 72BD may be easily modified to have a response time of less than 0.2 ms, but at the expense of decreasing its S/N ratio by a factor of 3.5.[10] However this additional noise is high-frequency noise, and can easily be filtered by the LIA. In the present study, no difference in the final LIA output S/N ratio was found whether using the capacitance meter as purchased or modified. Assuming that this meter can pass a pulse as narrow as 0.1 ms, it implies that in its modified form the smallest values for t_p and t_d are 0.1 and 0.2 ms, respectively, and hence $t_g = 0.3$ ms.

After having established the shortest allowed gate-off time (which is related to the maximum frequency), the second factor to be considered is the magnitude of the LIA output. As illustrated in Fig. 4, the normalized LIA output signal decreases due to measurements at higher frequencies. The maximum allowed decrease will depend on the magnitude of the DLTS signal, i.e., the concentration of the defects that cause the transient. For example, from Fig. 4 we see that in order for the normalized output signal to be more than 0.1 for $t_p = t_d = 0.4$ ms, the frequency should be less than 700 Hz. If the normalized output signal becomes less than this predetermined value of 0.1, it means that the S/N ratio may become so low that measurement errors are caused when determining the exact DLTS peak position.

Third, one has to decide whether or not to go to the trouble of numerically evaluating τ_{max}/T_0. If one chooses not to do so, then the maximum frequency for a predetermined allowed variation τ_{max}/T_0 may be found from calibration curves such as in Fig. 3, or in the special case where $t_p \cong 4t_d$, from Fig. 5.

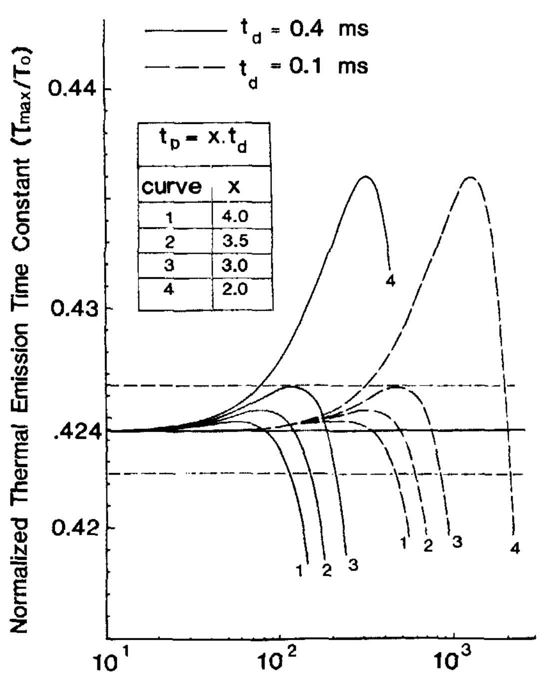

FIG. 5. Normalized maximum emission time constant τ_{max}/T_0 vs frequency for two sets of t_d values: 0.1 and 0.4 ms. For each t_d value, t_p values defined by $t_p = xt_d$ are drawn, with x between 2 and 4. The distance between the two broken lines parallel to $\tau_{max}/T_0 = 0.424$ represents a 1% change in the values of τ_{max}/T_0. Note that the τ_{max}/T_0 scale is eight times more sensitive than in Fig. 3.

B. Experimental work

As an illustration of the principles that have been developed, the characteristics of the E2 level in proton-bombarded GaAs was measured. The experimental data was recorded using a LIA based DLTS system with a Boonton 72BD capacitance meter which was modified to have a response time of less than 0.2 ms. The filling pulse amplitude and quiescent bias during these measurements were 1.4 and 1.0 V, respectively. As summarized in Table I, several different (t_p, t_d) combinations were used for which the maximum frequency was determined by the requirement that the normalized LIA output should be greater than 0.1. At measurements with t_d as low as 0.1 ms no observable variation in the calculated DLTS parameters due to false (system) transients were detected at frequencies as high as 2200 Hz.

The DLTS data for the E2 defect is plotted in the Arrhenius graph in Fig. 6. Because most of the data points for the different cases summarized in Table I lie very close together, only those for $t_p = 0.1$, $t_d = 0.2$ ms (with and without the t_p correction) and $t_p = 0.2$, $t_d = 0.3$ ms (without the t_p correction) are shown. The least-squares fits constructed by using the data points indicated by circles show that if τ_{max} is calculated by taking into account both t_p and t_d, then, irrespective of their values, all the experimental points lie on a straight line. However, as indicated by the squares and the diamond symbols in Fig. 6, a deviation from the straight line that increases with frequency and gate-of time is observed when ignoring the t_p in the numerical computation of τ_{max}. In fact, it was found that the experimental points obtained by neglecting both t_p and t_d and using $\tau_{max}/T_0 = 0.424$ lie closer to the straight line fit than when neglecting only t_p. This may be attributed to the manner in which the phase is set: the contributions to t_p and t_d "oppose" each other after being multiplied by the weighting function. Although not shown in Fig. 6, an excellent fit using $\tau_{max} = 0.424$ for all frequencies up to 500 Hz is obtained for $t_p = 4t_d = 0.6$ ms.

Table I lists the values of the defect properties obtained in the different temperature regions (above and below liquid-nitrogen temperature) for different t_p and t_d combina-

TABLE I. Defect characteristics of the E2 level in proton implanted GaAs

Gate-off times (ms)		Frequency range (Hz)	Temperature range (K)	$E_c - E_t$ (eV)			$\sigma_{maj} \times 10^{-13}$ (cm^2)		
t_p	t_d			A[a]	B[a]	C[a]	A[a]	B[a]	C[a]
0.1	0.2	2–50	69–79	0.143	0.143	0.143	1.0	1.0	1.0
		50–2000	79–94	0.144	0.149	0.148	1.3	2.7	2.4
		2–2000[b]	69–94	0.144	0.144	0.146	1.2	1.8	2.2
0.2	0.3	2–50	69–79	0.142	0.142	0.142	0.9	0.9	0.9
		50–1000	79–90	0.146	0.169	0.152	1.7	46	4.2
		2–1000	69–90	0.145	0.152	0.147	1.6	4.5	2.0
0.4	0.15	2–50	69–79	0.142	0.142	0.142	0.9	0.9	0.9
		50–500	79–88	0.150	0.147	0.148	2.8	2.0	2.3
		2–500	69–88	0.145	0.145	0.145	1.5	1.4	1.5

[a] A—both t_p and t_d accounted for, B—only t_d accounted for, C—both t_p and t_d ignored: $\tau_{max}/T_0 = 0.424$.
[b] At 1500 Hz: $t_d = 0.15$ ms, at 2200 Hz: $t_d = 0.1$ ms.

tions with and without the t_p correction. The activation energy and capture cross section obtained from the least-squares fit at frequencies of between 2 and 2200 Hz in Fig. 6 are $E_t = E_c - 0.144$ eV and $\sigma_{maj} = 1.2 \times 10^{-13}$ cm^2. These values agree well with those recently reported by Pons *et al.* for the E2 level, namely $E_t = E_c - 0.140$ eV and $\sigma_{maj} = 1.2 \times 10^{-13}$ cm^2. Note that there is an almost negligible deviation of the DLTS parameters from these values when calculating them by taking $\tau_{max} = 0.424$ up to frequencies of 1500 Hz for $t_p = 0.1$ and $t_d = 0.15$ ms and up to 1000 Hz for $t_p = 0.2$ and $t_d = 0.3$ ms. An important conclusion from the data above is that capacitance DLTS characterization of defects such as the E2 in GaAs, which is usually observed below 77 K at frequencies below 50 Hz, is possible when only a liquid-nitrogen cryostat is available. This is clearly illustrated in Fig. 6, where the data points to the left of the vertical broken line represent those that would be obtained in a liquid-nitrogen cryostat (above 80 K). For frequencies below 50 Hz, the DLTS peaks occur below 80 K, i.e., below the lowest temperature achieved in an average liquid-nitrogen cryostat. If measurements are made at frequencies between 50 and 2000 Hz, then τ_{max} values spanning more than an order of magnitude are obtained. As indicated in Table I, this facilitates a fairly accurate determination of the activation energy and capture cross section. Clearly, if both t_p and t_d are not included in the calculation of τ_{max} in this limited frequency range, then the errors in the calculated activation energy, and especially the capture cross section, are much larger than for the full frequency range. It is therefore concluded that levels such as the E2 can be characterized by capacitance DLTS at temperatures above that of liquid nitrogen as long as both t_p and t_d are accounted for in order that high enough frequencies may be used.

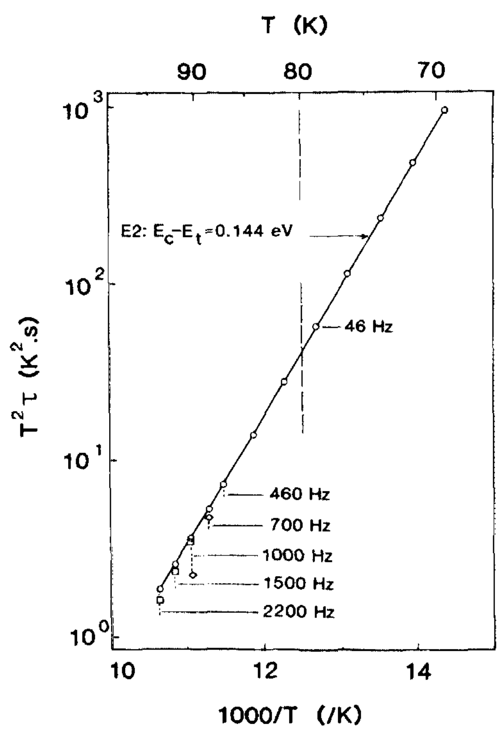

FIG. 6. Arrhenius plot of the DLTS data recorded at frequencies of between 2 and 2200 Hz for the E2 level in proton-implanted GaAs. ○ (t_p;t_d) = (0.1;0.2), both t_p and t_d accounted for; □ (t_p;t_d) = (0.1;0.2), only t_d accounted for; ◇ (t_p;t_d) = (0.2;0.3), only t_d accounted for. Where a symbol is omitted at frequencies above 1000 Hz, it coincided exactly with a circle at the corresponding frequency. Data points to the left of the broken vertical line are typical of those that would be obtained in liquid-nitrogen cryostat.

III. CONCLUSIONS

From the preceding analysis and calculations it is evident that both the pulse width t_p and the capacitance meter response time t_d affect the calculated values of the maximum emission decay time constant τ_{max}. It was found that the value of $\tau_{max}/T_0 = 0.424$ frequently used to determine τ_{max} for different frequencies during DLTS experiments, generally differs from the calculated value of τ_{max}/T_0 by more than 1% and 5% for frequencies above $0.04/t_g$ and $0.1/t_g$, respectively. For the exceptional cases where $3t_d \leqslant t_p \leqslant 4t_d$, this approximation is valid at frequencies up to $0.2/t_g$. The errors introduced when neglecting either t_p or t_d in the calculation of τ_{max} noticeably influenced the activation energy and capture cross section of the E2 level in proton-implanted

GaAs calculated from a plot of $\tau_{\max} T^2$ vs $1000/T$ if the total gate-off time $t_g = t_p + t_d$ became greater than about 0.2 times the LIA period T_0. In fact, when neglecting only t_p these errors are larger than those introduced when neglecting both t_p and t_d, and simply using the approximation $\tau_{\max}/T_0 = 0.424$.

Probably the most important consequence of this study is that accurate lock-in amplifier DLTS measurements using a modified 1-MHz capacitance meter are possible at frequencies up to and above 2000 Hz, provided both the pulse width and delay times are numerically accounted for when calculating $\tau_{\max}$. This increases the conventional LIA method's frequency range by about an order of magnitude. This extended frequency range for DLTS measurements is important because it facilitates characterization of defects which, at frequencies below 50–100 Hz, exhibit DLTS peaks slightly below 77–80 K, the lowest temperature of typical liquid-nitrogen cryostats. As the frequency is increased to above 50–100 Hz, the DLTS peaks appear at higher temperatures, which may be above the lowest temperature of the liquid-nitrogen cryostats, and thus may be observed and characterized. This was illustrated for the radiation-induced E2 level in GaAs. As may be expected, when neglecting t_p or t_d the errors in the activation energy and capture cross section become larger when only this upper part of the frequency range (50–2000 Hz) is used.

ACKNOWLEDGMENTS

The author would like to thank Dr. A. W. R. Leitch for helpful discussions and for critically reading the manuscript, as well as M. Nel for fabricating the Schottky barrier diodes used for this study.

APPENDIX

After defining

$$\xi = T_0/2\tau_{\max},$$
$$\alpha = 2t_g/T_0,$$
$$\beta = 2t_d/T_0,$$
$$A = \exp(-2\xi),$$
$$B = \exp(-\beta\xi),$$
$$C = \exp(\alpha\xi),$$
$$D = \exp(2\xi) = 1/A,$$
$$E = (\pi^2 + \xi^2)^{-1},$$
$$F = \cos\alpha\pi,\ G = \sin\alpha\pi,$$
$$J = C(F - \xi G/\pi) - D,$$
$$L = C[1 - \xi G/\pi + \xi^2(1-F)/\pi^2] - D,$$
$$M = \xi J I + \pi L F,$$
$$M' = dM/d\xi = \xi J I + \pi F, \tag{A1}$$

the LIA response in Eq. (10) can be written as

$$S_{\exp} = 2T_0 ABEM. \tag{A2}$$

By using Eqs. (A1) and (A2), the condition for a maximum LIA signal at the DLTS peak as given in Eq. (11) becomes

$$f(\xi) = 2M(1 + \beta/2 + \xi E) - M' = 0. \tag{A3}$$

Equation (A3) is nonlinear in ξ and has to be solved numerically. This may be done iteratively by using one of several algorithms, of which the Newton–Raphson method is probably the most well known. In this method the $(i+1)$th value for ξ, ξ_{i+1}, is obtained from

$$\xi_{i+1} = \xi_i - f(\xi)/f'(\xi). \tag{A4}$$

Here, $f'(\xi) = df(\xi)/d\xi$ is obtained from Eqs. (A1) and (A2) as

$$f'(\xi) = 2M'(\beta/2 + \xi E) + 2ME(-2\xi^2 E + 1). \tag{A5}$$

In solving Eq. (A3) by using (A4), the first estimate ξ_0 is chosen as 0.424 T_0, and thereafter convergence is usually obtained within less than five iterations.

[1] D. V. Lang, J. Appl. Phys. **45**, 3023 (1974).
[2] G. L. Miller, J. V. Ramirez, and D. A. H. Robinson, J. Appl. Phys. **46**, 2638 (1975).
[3] L. C. Kimerling, IEEE Trans. Nucl. Sci. **NS-23**, 1497 (1976).
[4] Polaron DLTS system, marketed by Polaron Equipment Limited, 53-63 Greenhill Crescent, Watford Business Park, Watford Hertfordshire WD1 8XG, U.K.
[5] M. Okuyama, H. Takakura, and Y. Hamakawa, Solid-State Electronics, **26**, 689 (1983).
[6] D. S. Day, M. Y. Tsai, B. G. Streetman, and D. V. Lang, J. Appl. Phys. **50**, 5093 (1979).
[7] G. L. Miller, D. V. Lang, and L. C. Kimerling, Ann. Rev. Mater. Sci. **7**, 377 (1977).
[8] D. Pons, P. M. Mooney, and J. C. Bourgoin, J. Appl. Phys. **51**, 2038 (1980).
[9] J. T. Schott, H. M. DeAngelis, and W. R. White, Airforce Cambridge Laboratories Report No. AFCRL-TR-76-0024, 1976.
[10] T. I. Chappell and C. M. Ransom, Rev. Sci. Instrum. **55**, 200 (1984).
[11] D. Pons and J. C. Bourgoin, J. Phys. C **18**, 3839 (1985).